Multiple-Band Trigger Features of Midbrain Auditory Neurons Revealed in Composite Spectro-Temporal Receptive Fields

T.W. Chiu[1]* and Paul W.F. Poon

[1]*Institute of Basic Medical Science, and Department of Physiology*
Medical College, National Cheng Kung University
Tainan 701, Taiwan, R.O.C.

Abstract

Receptive fields of single units in the auditory midbrain of anesthetized rats were studied using random FM-tone stimuli of narrow frequency-ranges. Peri-spike averaging of the modulating waveform first produced a spectro-temporal receptive field (STRF). Combining STRFs obtained from the same unit at different frequency regions generated a composite receptive field covering a wider frequency range of 2 to 3 octaves. About 20% of the composite STRFs (26/122) showed a pattern of multiple-bands which were not clear in the non-composite maps. Multiple-bands in a given composite map were often oriented in the same direction (representing upward or downward FM ramp) separated at rather regular frequency intervals. They reflect multiple FM trigger features in the stimulus rather than repetitive firing to a single trigger feature. Results showed that the subcortical auditory pathways are capable of detecting multiple FM features and such sensitivity could be useful in detecting multiple-harmonic FM bands present in the vocalization sounds.

Key Words: **inferior colliculus, frequency modulation, STRF, trigger feature, vocalization sound**

Introduction

What stimulus feature in the complex sound auditory neurons would best respond to is a fundamental question in understanding neural coding of complex sounds (45). A number of studies have been made to determine the trigger features of central auditory neurons particularly with reference to time-varying features that characterize many speech sounds. Hermes *et al.* (17) were the first to present white noise to evoke spike responses from auditory units and by the technique of reverse correlation, reconstructed stimulus features time-locked to the evoked neural spikes. The result, plotted on the time-frequency plane, is known as a spectro-temporal receptive field (STRF) of the neuron (1, 2, 5, 8, 9, 15, 20, 27). Others used more complicated stimuli like random chords, dynamic ripple noise, or even natural sounds (6, 7, 13, 21, 37, 38, 42). These methods are similar in nature to the original white noise approach in using random stimuli coupled with spike-triggered averaging. More recently, the use of a random frequency modulated (FM) tone to produce STRF has been shown to work with great efficacy (3, 18, 33). The random FM tone is generated as follows: a low-pass filtered white noise is fed to the voltage-to-frequency input of a sine-wave generator to produce the acoustic signal. The voltage of the time-varying waveform dictates the instantaneous frequency of the sine-wave and results in a random FM tone. Averaging or overlaying the pre-spike modulating waveforms (rather than the acoustic waveform *per se*) yields a STRF within a period of data collection as brief as 2 min. Each of the above methods has its own merits and shortcomings. For example, the method of random chord stimulation can reveal inhibitory areas in the receptive field but the data collection is more time-consuming. On the other hand the method of random FM stimulation is faster but it fails to reveal the inhibitory areas. The latter method would be adequate in studies when only the

Corresponding author: Dr. Paul W.F. Poon, Department of Physiology, Medical College, National Cheng Kung University, 1 University Road, Tainan 70101, Taiwan, R.O.C. Fax: +886-6-2362780, E-mail: ppoon@mail.ncku.edu.tw
*Present address: Department of Psychology, University of Washington, Seattle, WA, USA.
Received: April 26, 2006; Revised: November 10, 2006; Accepted: November 13, 2006.

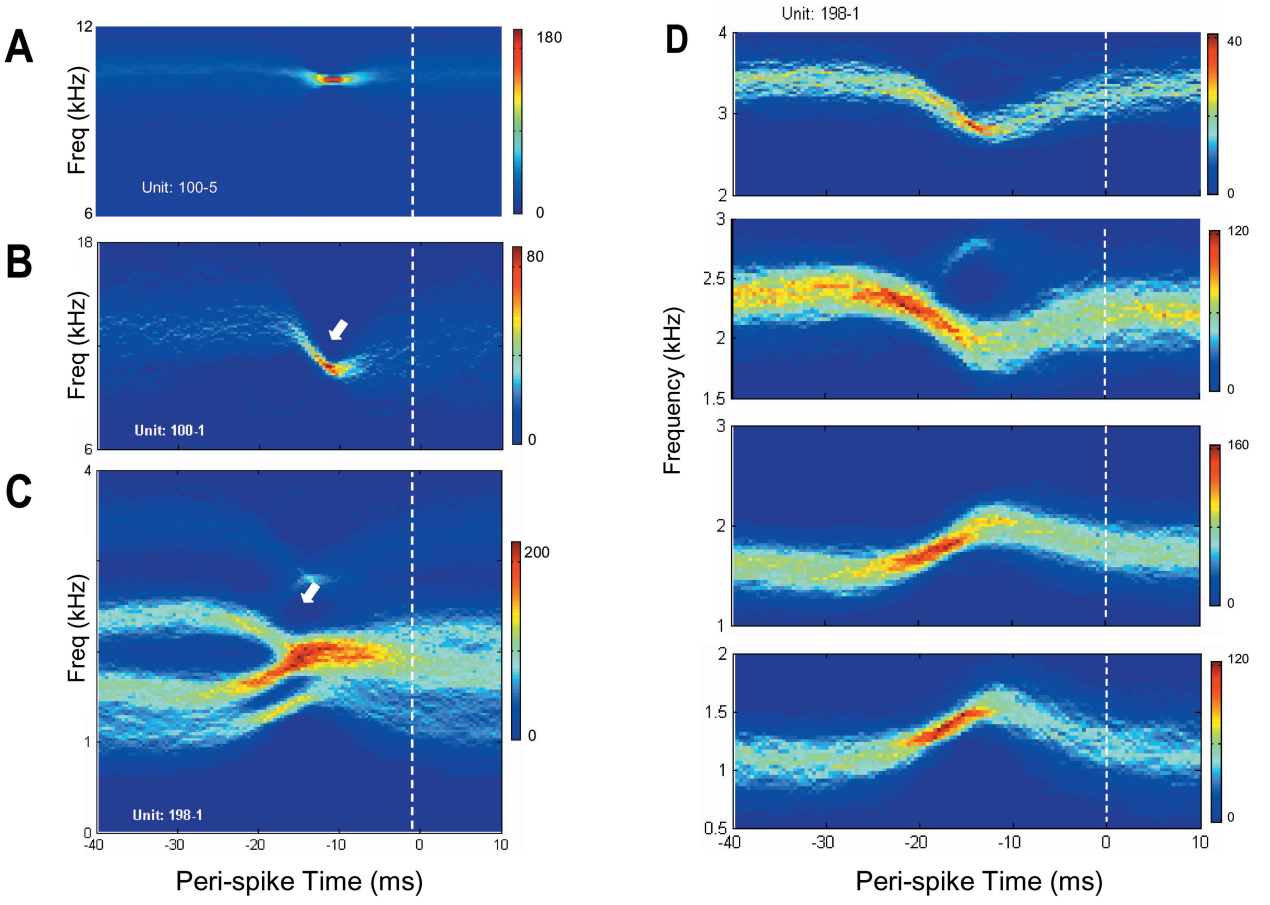

Fig. 1. Examples from three IC cells showing (A): STRF of an "FM-insensitive" unit, (B): single-band STRF of an "FM-sensitive" unit, (C): multiple-band STRF of an "FM-sensitive" unit (in composite plot), and (D): same cell as in (C) showing the individual STRFs that are used to form the composite plot by frequency and time overlay. Note the systematically varied frequency ranges and the spectral overlap across STRFs. The count at each pixel is color-coded (see scales on the right) to reflect the degree of overlap in the modulating waveform preceding the spike. Spike occurrence is aligned at peri-spike time zero (vertical dashed line). Each STRF is the result of summing 800 to 2,000 modulating waveforms. Arrows indicate area of low probability of waveform overlap, suggesting the presence of inhibitory areas. Note the difference in frequency scale across panels.

excitatory responses are of interest.

These studies are often designed to determine the "trigger" features of central auditory neurons given a complex sound stimulus. "Trigger feature" is operationally useful in characterizing stimulus-coding of central neurons. The term "trigger" was first used in studies of other non-auditory systems. It referred to the robust responses evoked from a neuron after presenting specific stimulus feature (25, 28, 44). The term "trigger feature" is closely related in concept to "feature selectivity" (6) and "receptive space" (31, 32). In reference to trigger features, the probabilistic nature of neural response to identical stimulus is often acknowledged (3) and the neural circuitry under study is assumed to behave like a linear system.

FM signals are one of the trigger features as they are present in vocalization sounds of many animal species (11, 16, 29, 36). In human, FM components are known to be important for speech recognition (19). It is therefore not surprising that FM sensitive cells are commonly found in the auditory system (12, 14, 22, 31, 34, 35). For example, about 1/3 of units found in the inferior colliculus (IC) are driven by FM but not by pure tones (31). The IC is also the first nuclear station in the ascending auditory system where FM specialized responses emerge in a substantial proportion (10). However, the reported proportion of FM sensitive neurons in the auditory system varies across laboratories due to differences in experimental procedure and in the definition of FM-sensitivity (14, 31, 34, 39). In general, the FM-specialized cells increase in proportion from brainstem towards cortex, according to a finding that supports the importance of FM sensitivity in coding complex sounds (40).

In a typical STRF of a FM-sensitive neuron obtained with random FM tone, there is a dense overlap of the modulating waveforms preceding the occurrence of spikes. In spite of neural response jitter

(3), this dense overlap forms a visible band-like structure in the receptive field (*e.g.*, Fig. 1A). The band-like structure is typically oriented at an angle to the time axis, representing an FM trigger feature for the cell. For most IC units, such FM features precede spike occurrence at latencies consistent with the central transmission time of about 8-12 msec as measured from the cochlea to the IC (3, 33, 43). Using such an approach, single-band STRF was revealed for the overwhelming majority of IC units (33), whereas in the primary auditory cortex, some multiple-band STRFs have been reported using dynamic ripple noise as stimulus (7, 13, 21, 38). Knowledge on the subcortical processing of multiple-band FM stimuli is missing; however, it is obviously important in understanding the coding of speech sound.

In this study, we determined STRFs of FM-sensitive cells in the auditory midbrain using random FM-tone stimuli. For a given cell we first obtained a series of STRFs with partial overlap in frequency range and STRFs were subsequently combined to form a composite map. We found multiple-band patterns in as many as 21% of the STRFs.

Materials and Methods

Animal Preparation

Young adult rats (Sprague-Dawley, body weight: 150-300 gm) were used. Anesthesia was induced by Urethane (Sigma, 2.0 gm/kg b.w., i.p.) and maintained with supplementary doses when needed (0.5 gm/kg b.w., i.p.). Tracheal secretion was reduced by Robinul (Robins, 0.02 mg/ml, 0.05 mg/kg b.w., s.c.). Craniotomy exposed the occipital lobe on one side, followed by gentle aspiration of the cortex to visualize the underlying IC. Cerebrospinal fluid was drained at the foramen magnum to minimize brain pulsation. A screw was cemented onto the frontal skull for subsequent fixation to a special head holder to facilitate free-field acoustic stimulation. The skin incision was partially sutured to restore the pinnae back to their resting positions. Rectal temperature was controlled at 38 ± 0.5°C by a thermal pad. During recording, the animal was placed inside a sound room (1.8 × 2.45 × 2.28 m, Height × Width × Length, Industrial Acoustic Co. Winchester, UK), the inner wall of which was lined with corrugated foam to reduce sound reflections. The acoustic insulation of the room was > 40 dB from 0.5 to 40 kHz. The experiment was remotely controlled from outside the sound room.

Acoustic Stimulation

The "random" modulating signals were digitally generated (HP Workstation E4). First, a wide-band noise signal (100 kHz) was low-pass filtered (6 dB/octave roll-off) at a cut-off frequency of 12.5, 25 or 125 Hz. FM stimuli of this kind have been shown to be effective in exciting FM cells in the rat IC (33). A computer interface (Tucker Davis Technologies DD1) was used to deliver the stimulus and collect spike responses. Acoustic signals were amplified (QUAD 306) and fed into a free field speaker (Pioneer SP77) placed 70 cm in the horizontal plane 30° in azimuth contralateral to the exposed IC. This placed the sound source in the general direction of the acoustic axis for maximal sound effects. The overall frequency response of the audio system was within ±12 dB from 0.4 to 40 kHz as measured with a calibration microphone (Bruel & Kjaer 4191) at the head of the animal.

Electrophysiology

Single unit activities were recorded extracellularly with a glass micropipette filled with 3 M KCl solution and some with additional 2% Pontamine sky blue (impedance: 30-60 MΩ). The electrode explored the IC at multiple steps of 1-3 μm as controlled by a motorized microdrive (Narishige 5113). The unit activity was amplified (Axonprobe-1A, Princeton Applied Research C-5113) and band-pass filtered at 0.3 to 3.0 kHz to improve signal-to-noise ratio. Unit activities were monitored audio-visually according to the conventional procedure of extracellular recordings. Finally, single spikes were conditioned into 0.5 msec rectangular pulses using a level discriminator and their time of occurrence stored in the computer for off-line analysis.

At the end of experiment, electrophoretic injection of Pontamine sky blue (-3 μA for 5 min) was made to mark the location of the last recording site. Histological verification of recording site was done by sectioning the brain at 40 μm on a freezing microtome and examining the dye injection sites under microscope (details see reference 30).

Generation of STRF

After an auditory responsive unit had been identified by its response to an intense click (90 dB SPL, 0.1 msec duration), its best frequency (BF) and minimum threshold (MT) to steady tone stimuli were determined. Responses to the 3 random FM stimuli were recorded at a level 30 dB above its MT with center frequency set near the unit's BF. Only the dataset with best total spike count to the 3 random FM stimuli was analyzed. Each dataset contained a total of 60 trials (each of 2 sec long). Neural spikes, after being conditioned into rectangular pulses, were digitized concurrently with the modulating waveforms. The peri-spike modulating waveforms (40 msec pre-, to 10 msec post-spike) were extracted and summed pixel-

by-pixel in the time-versus-frequency plane. The density of waveform overlap was further color-coded for visualization of overlapping regions in the STRF. The next center frequency of the random FM stimulus was varied systematically from low to high with 30 to 50% overlap between adjacent STRFs (see example in Fig. 1D). For any given unit, 4 to 5 STRFs were generated at different carrier frequencies covering the neighboring regions of its BF. STRFs were then combined to produce a composite map of STRF (Fig. 1B). This procedure involved alignment of adjacent STRFs along the frequency axis and then summing the results pixel-by-pixel. The frequency range in the composite STRFs normally covered 2 to 3 octaves around the BF of the unit, enough to reveal most bands in the STRF.

Generation of Response Area (RA)

Here we used a large-range but slow FM sweep as stimulus. The instantaneous frequency was varied exponentially from 1 to 10 or 1 to 60 kHz, representing a frequency range of 3.3 or 5.9 octaves with the stimulus level varied systematically across 2-sec trials (Fig. 2B). By plotting the spike response of the unit as a dot raster, we characterized the unit's sensitivity to tone stimuli as a function of instantaneous frequency and intensity, or its response area (RA) (details see reference 4).

Experimental procedures were approved by the Animal Ethics Committee of the National Cheng Kung University.

Results

We studied a total of 291 units in 32 rats. All the dye-injected sites were found within the central and external divisions of the IC. The ranges of BF and MT of these units were respectively 1 to 60 kHz and -20 to 75 dB SPL, covering the normal audiogram of the rat. The 3 random FM stimuli effectively activated about 3/4 of the auditory units (n = 217) that were driven by the hunting click signal. Table 1A shows the distribution of units in 3 categories based on their responses to FM and pure tones. About 40% of the units (n = 112) responded to random FM but not to pure tone (we called "FM-specialized" cells, see reference 31). About 35% (n = 105) responded to both random FM and pure tone ("FM-mixed" cells). The remaining 25% responded only to pure tone ("FM-insensitive" cells). The statistics were comparable to a previous report on a larger population (31) indicating a rather even sampling of the IC.

In 217 IC units (75% of sample) that had responded to FM stimuli, 56% of them (n = 122) displayed clear band-like structures in their receptive fields. These

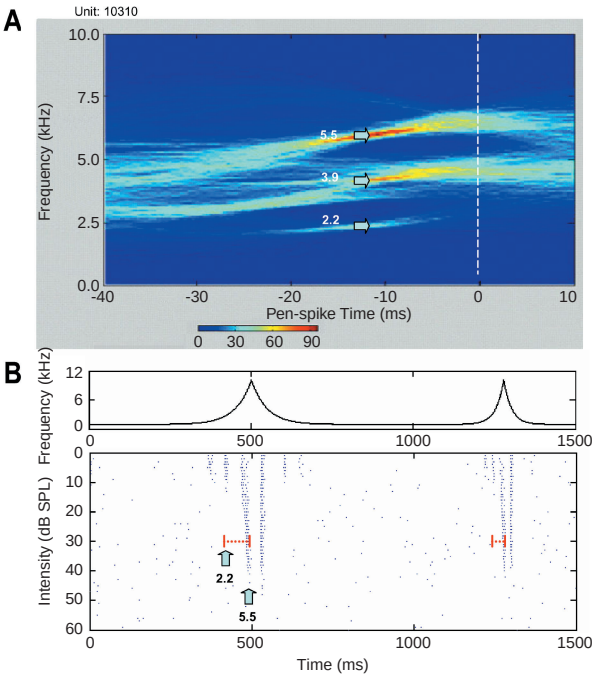

Fig. 2. Comparison of STRF and RA of the same cell. (A): multiple-band STRF showing the regular intervals between adjacent bands. (B): RA obtained with two different exponential tone sweeps (frequency was varied from 1 to 10 kHz in 0.5 or 0.25 sec, with intensity varied systematically across trials from top to bottom). Upper panel shows the exponential waveforms depicting the instantaneous frequency of the slow FM tone. Lower panel shows the corresponding spike responses in response to the two exponential FM stimuli (each action potential is represented by a dot). Arrows: frequency marks in kHz. Note regular intervals between arrows in (A) and vertical strip spike response pattern in (B). For comparison the red dashed lines in (B) mark the stimulus level and frequency range of the random FM used in obtaining the STRF in (A). For simplicity, the dashed lines are shown only on the rising phase of the exponential tone-sweep.

STRFs were further analyzed. About half of them (63/122, 52%) belonged to the subpopulation of "FM-specialized" cells, and the other half (59/122, 48%) belonged to the subpopulation of "FM-mixed" cells.

Two general patterns of STRF were found, *viz.*, (a) single-band (*e.g.*, Fig. 1B), or (b) multiple-band (*e.g.*, Fig. 1C). More multiple-bands STRFs were found in the "FM-mixed" subpopulation than the "FM-specialized" (31% versus 11%, Table 1B). The majority of composite STRFs (96/122, 79%,) showed single-band patterns. The upward or downward FM bands occurred at almost equal chances (51% versus 49%). Occasionally, there were two bands, one upward and one downward FM crossing each other at the BF (appearing in a shape like a cross in the STRF map.)

Table 1

A: Classification of IC units according to their responses to pure tones or random FM tones (n = 291 cells in 32 rats).

Cell type	Stimulus		No. of cells (% of total)
	Pure tone	FM tone	
"FM specialized"	–	+	39% (n = 112)
"FM-mixed"	+	+	36% (n = 105)
"FM insensitive"	+	–	25% (n = 74)
No. of cells (% of total)	62% (n = 179)	75% (n = 217)	100% (n = 291)

B: Relative proportions of single or multiple-band STRF in "FM-specialized" and "FM-mixed" cells that showed clear bands in their STRFs (n = 112 cells).

"FM-specialized" cells (n = 63)	Single-band STRF	Multiple-band STRF
No. of cells (% of subpopulation)	55 (88%)	8 (11%)
"FM-mixed" cells (n = 59)	Single-band STRF	Multiple-band STRF
No. of cells (% of subpopulation)	41 (69%)	18 (31%)

For the sake of simplicity, we classified this cross-pattern of STRF as single-band in this study. Upward and downward FMs were found across almost all BFs. There is no difference between the mean BFs of upward-FM and downward-FM units (mean ± SD: 11.8 ± 11.8 versus 13.7 ± 8.5, $P = 0.39$, Student's *t*-test).

A smaller but substantial number of composite STRFs (26/122, 21%) showed two or more bands (mean ± SD = 2.3 ± 0.5) (Fig. 1C). We classified them as "multiple-band" STRFs according to the definition that at least two of the bands appeared in the same orientation. Again, both upward and downward bands were found. Furthermore, there was a mixture of upward and downward FM bands especially for "FM-mixed" cells. The highest number of bands we found was 5. In terms of response sensitivity, the mean MT of multiple-band units was similar to that of single-band units (mean ± SD: 48.2 ± 27.0 versus 45.9 ± 20.8, $P = 0.65$, Student's *t*-test). For comparison, the STRF of "FM-insensitive" unit is also shown in Fig. 1A.

For the subpopulation multiple-band units, we also examined the band pattern in their individual STRFs. Since these individual STRFs form the basis of the composite map. As shown in Fig. 1D (the same unit as in Fig. 1C), the STRFs obtained at a narrow spectral range systemically varied across frequency produce pictures each of which we would have classified as single-band according to our criteria. Nearly half of those units that we had eventually classified as multiple-band (12/26, 46%) showed single-band in the non-composite map. Hence, the approach of composite map has doubled the chance of revealing multiple-band units in the IC.

The relationship between adjacent bands in the composite STRFs was further examined. The multiple frequency bands in the STRF often appeared in rather regular intervals. In Fig. 2A, three bands were found at 2.2, 3.9, 5.5 kHz with an inter-band interval of 1.6 kHz.

For those units with multiple-band STRF particularly in the subpopulation of "FM-mixed" cells, we were also able to compare band patterns in STRF with their responses to more steady tones as expressed in terms of response area (RA). At such a slow and long FM sweep, similar multiple-band responses occurred in the form of vertical strips of response in the dot raster within comparable frequency ranges of the STRF. However, there was no exact correspondence to the STRF band patterns. Figure 2 shows an example of a comparison between STRF and the corresponding RA of a cell. First the band patterns in RA and STRF though occupied comparable frequency ranges were obviously different from each other. Second, their respective thresholds of response were also different. For example, at the intensity of 30 dB SPL (dashed lines in Fig. 2B, lower panel) the RA shows only a

weak response to a tone with frequency modulated around 5.5 kHz. At the same level of stimulation, a multiple-band pattern appears in the STRF. Responses to falling phases of the tone sweep found mainly at low sweep rates drop at increased sweep rates (Fig. 2B). We often observed in other multiple-band units a reduction in spike responses when the frequency range of the random FM stimulus was intentionally expanded. Results showed that the STRF obtained with narrow frequency-range stimuli cannot be accurately predicted by the response pattern in the RA.

Discussion

In the present study, a substantial proportion of STRFs (21%) in IC are multiple-band as revealed by compositing STRFs of narrow-frequency ranges. This proportion is the highest reported so far, compared with a reduction to half (10%) of multiple-band units if judged solely by non-composite STRF. Since our results of multiple-band STRFs were obtained using a mono-tone stimulus, the proportion of multiple-band units actually existed at the IC may still be under-estimated. For example, for units that require simultaneous multiple-FM tones as trigger feature, they would not be activated by our mono-tone stimulus. Multiple-band units described here are not the same as "combination-sensitive" neurons as reported at the IC and the auditory cortex of the echo-locating bat (25, 41). The approach of reverse correlation used here would fail to detect such nonlinear response properties since the response to the simultaneous presence of two different tones is not a linear sum of the energy at their respective frequencies. Regardless of this, our results suggested that such multiple-band units, by virtue of their substantial proportion in the auditory midbrain, could play a more important role in coding complex sounds than previously thought.

Band features in individual STRFs merge well with one another in the composite map. This suggested that the neural system under study behaved grossly in a linear fashion to the monotone stimulus. If the system behaves nonlinearly, the individual bands obtained at different carrier frequencies would fail to merge in the composite map. This finding also justified the use of composite maps to reveal FM trigger features. However, one cannot exclude the possibility that non-linear interactions may occur especially at the cortex when more tones were presented simultaneously (24).

The present method of getting at the receptive fields of auditory neuron results in a different picture than those revealed using a single large-range FM stimulus. Specifically, there are more trigger features found in the STRF than in the RA, a finding that is consistent with a greater sensitivity to the random FM

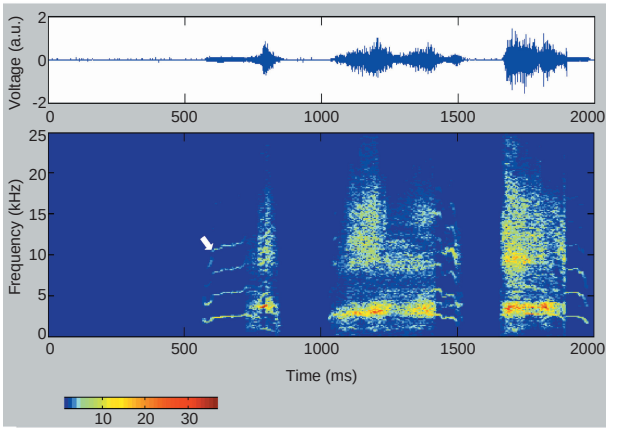

Fig. 3. Rat vocalization sounds showing the time waveform (top panel, y-axis in arbitrary unit) and the corresponding spectrogram (bottom panel) of a 2-sec sample. The spectrogram, obtained using short-time Fourier Transforms, is color-coded to represent energy levels of the frequency components (see scale bar at bottom, arbitrary unit). Note the presence of multiple harmonics or multiple FM components in the form of parallel bands (*e.g.* arrow).

tone. The discrepancy in results could also be related to the presence of un-revealed inhibition. Inhibitory side-bands are well known to exist in IC (23). Inhibitory areas flanking the upper and lower bounds of an FM band have been reported in the STRF of auditory cortex (6). Similarly inhibitory area was also used in successful modeling of the STRF of FM-specialized cells (18). In the present study some areas of the STRF next to the band-like structure show exceptionally low probability of modulating waveform, consistent with the presence of inhibitory areas (*e.g.*, arrows in Fig. 1B-C). Our finding of a greater proportion of multiple-band STRFs could be related to the method of splitting the wide-range stimulus into narrower FM tones before combining results into composite STRFs for evaluation. It is likely that random FM signals of narrow- but not large-ranges have a greater chance of avoiding the inhibitory areas especially those located above and below the excitatory fields in the STRF. This narrow-range FM stimulus, by virtue of its similarity to the spectral pattern present in the vocalization sound (Fig. 3) could well account for its greater excitability of IC neurons.

The sensitivity to dynamic ripples or natural sounds reported at the auditory cortex (7, 21, 38, 42) could reflect an FM sensitivity already existed at the midbrain. We noticed that the regular frequency intervals separating the various bands in the STRF bear a striking similarity with the multiple harmonic structures found in the rat vocalization sounds (Fig. 3). It is tempting to speculate that the presence of

multiple-band in the STRF could form the basis for detecting multiple harmonic components in the vocalization sounds. We have preliminary data to show that FM-specialized cells often responded vigorously to the vocalization signal where multiple-band features are present. Detailed comparison of inter-band intervals in both the STRF and the vocalization sound would lie beyond the scope of the present study as we have not yet fully considered other response determinants like stimulus levels.

Acknowledgments

We thank Prof. Pete Casseday for his comments and Prof. Xinde Sun for his helpful inputs at the initial stage of experiment; supported in part by National Science Council, Taiwan, ROC.

References

1. Aertsen, A.M. and Johannesma, P.I. The spectro-temporal receptive field. A functional characteristic of auditory neurons. *Biol. Cybernet*. 42: 133-143, 1981a.
2. Aertsen, A.M. and Johannesma, P.I. A comparison of the spectro-temporal sensitivity of auditory neurons to tonal and natural stimuli. *Biol. Cybernet.* 42: 145-156, 1981b.
3. Chang, T.R., Chung, P.C., Chiu, T.W. and Poon, P.W.F. A new method for adjusting response jitter in the STRF obtained by spike-trigger averaging. *Biosystems* 79: 213-222, 2005.
4. Chiu, T.W., Liu, Y.D. and Poon, P.W.F. Transient frequency and intensity sensitivities of central auditory neurons estimated with sweep tone - a new approach. *Chinese J. Physiol*. 41: 133-138, 1998.
5. Clopton, B.M. and Backoff, P.M. Spectrotemporal receptive fields of neurons in cochlear nucleus of guinea pig. *Hearing Res.* 52: 329-344, 1991.
6. deCharms, R.C., Blake, D.T. and Merzenich, M.M. Optimizing sound features for cortical neurons. *Science* 280: 1439-1443, 1998.
7. Depireux, D.A., Simon, J.Z., Klein, D.J. and Shamma, S.A. Spectro-temporal response field characterization with dynamic ripples in ferret primary auditory cortex. *J. Neurophysiol*. 85: 1220-1234, 2001.
8. Eggermont, J.J., Aertsen, A.M. and Johannesma, P.I. Quantitative characterization procedure for auditory neurons based on the spectro-temporal receptive field. *Hearing Res*. 10: 167-190, 1983a.
9. Eggermont, J.J., Aertsen, A.M. and Johannesma, P.I. Prediction of the responses of auditory neurons in the midbrain of the grass frog based on the spectro-temporal receptive field. *Hearing Res*. 10: 191-202, 1983b.
10. Eggermont, J.J. Between sound and perception: reviewing the search for a neural code. *Hearing Res*. 157: 1-42, 2001.
11. Ehret, G. and Riecke, S. Mice and humans perceive multiharmonic communication sounds in the same way. *Proc. Natl. Acad. Sci. USA* 99: 479-482, 2002.
12. Erulkar, S.D., Nelson, P.G. and Bryan, J.S. Experimental and theoretical approaches to neural processing in the central auditory pathway. In: Contributions to sensory physiology, edited by Neff, W.D., Academic Press, New York, 1968, Vol. 3. pp. 149-189.
13. Escabi, M.A. and Schreiner, C.E. Nonlinear spectrotemporal sound analysis by neurons in the auditory midbrain. *J. Neurosci*. 22: 4114-4131, 2002.
14. Flesheim, C. and Oswald, J. Responses to exponential frequency modulations in the rat inferior colliculus. *Hearing Res*. 98: 137-151, 1996.
15. Fritz, J., Elhilali, M. and Shamma, S. Active listening: task-dependent plasticity of spectrotemporal receptive fields in primary auditory cortex. *Hearing Res*. 206: 159-176, 2005.
16. Heil, P. and Scheich, H. Spatial representation of frequency-modulated signals in the tonotopically organized auditory cortex analogue of the chick. *J. Comp. Neurol.* 322: 548-565, 1992.
17. Hermes, D.J., Aertsen, A.M., Johannesma, P.I. and Eggermont, J.J. Spectro-temporal characteristics of single units in the auditory midbrain of the lightly anaesthetised grass frog (Rana temporaria L) investigated with noise stimuli. *Hearing Res*. 5: 147-178, 1981.
18. Kao, M.C., Poon, P.W. and Sun, X. Modeling of the response of midbrain auditory neurons in the rat to their vocalization sounds based on FM sensitivities. *Biosystems* 40: 103-109, 1997.
19. Kay, R.H. Hearing of modulation in sounds. *Physiol. Rev*. 62: 894-969, 1982.
20. Kim, P.J. and Young, E.D. Comparative analysis of spectro-temporal receptive fields, reverse correlation functions, and frequency tuning curves of auditory-nerve fibers. *J. Acoust. Soc. Am*. 95: 410-422, 1994.
21. Klein, D.J., Depireux, D.A., Simon, J.Z. and Shamma, S.A. Robust spectrotemporal reverse correlation for the auditory system: optimizing stimulus design. *J. Comput. Neurosci*. 9: 85-111, 2000.
22. Lee, H.J., Wallani, T. and Mendelson, J.R. Temporal processing speed in the inferior colliculus of young and aged rats. *Hearing Res.* 174: 64-74, 2002.
23. Lu, Y. and Jen, P.H.S. GABAergic and glycinergic neural inhibition in excitatory frequency tuning of bat inferior collicular neurons. *Exp. Brain Res*. 141: 331-339, 2001.
24. Machens, C.K., Wehr, M.S. and Zador, A.M. Linearity of cortical receptive fields measured with natural sounds. *J. Neurosci*. 24: 1089-1100, 2004.
25. Munro, P.W. A model for generalization and specification by single neurons. *Biol. Cybernet*. 51: 169-179, 1984.
26. Nataraj, K. and Wenstrup, J.J. Roles of inhibition in creating complex auditory responses in the inferior colliculus: facilitated combination-sensitive neurons. *J. Neurophysiol*. 93: 3294-3312, 2005.
27. Nelken, I., Kim, P.J. and Young, E.D. Linear and nonlinear spectral integration in type IV neurons of the dorsal cochlear nucleus. II. Predicting responses with the use of nonlinear models. *J. Neurophysiol*. 78: 800-811, 1997.
28. Nelson, R.J. Responsiveness of monkey primary somatosensory cortical neurons to peripheral stimulation depends on 'motor-set'. *Brain Res.* 304: 143-148, 1984.
29. Ostwald, P. The sounds of infancy. *Dev. Med. Child Neurol*. 14: 350-361, 1972.
30. Poon, P.W.F., Chen, X. and Cheung, Y.M. Differences in FM responses correlate with morphology of neurons in the rat inferior colliculus. *Exp. Brain Res*. 91: 94-104, 1992.
31. Poon, P.W.F., Chen, X. and Hwang, J.C. Basic determinants for FM responses in the inferior colliculus of rats. *Exp. Brain Res.* 83: 598-606, 1991.
32. Poon, P.W.F. and Chiu, T.W. Similarities of FM and AM receptive space of single units at the auditory midbrain. *Biosystems* 59: 229-237, 2000.
33. Poon, P.W.F. and Yu, P.P. Spectro-temporal receptive fields of midbrain auditory neurons in the rat obtained with frequency modulated stimulation. *Neurosci. Lett.* 289: 9-12, 2000.
34. Rees, A. and Moller, A.R. Responses of neurons in the inferior colliculus of the rat to AM and FM tones. *Hearing Res.* 10: 301-330, 1983.
35. Ricketts, C., Mendelson, J.R., Anand, B. and English, R. Responses to time-varying stimuli in rat auditory cortex. *Hearing Res.* 123: 27-30, 1998.
36. Sales, G.D. Ultrasound and aggressive behaviour in rats and other small mammals. *Animal Behav*. 20: 88-100, 1972.
37. Schafer, M., Rubsamen, R., Dorrscheidt, G.J. and Knipschild, M.

Setting complex tasks to single units in the avian auditory forebrain. II. Do we really need natural stimuli to describe neuronal response characteristics? *Hearing Res*. 57: 231-244, 1992.
38. Sen, K., Theunissen, F.E. and Doupe, A.J. Feature analysis of natural sounds in the songbird auditory forebrain. *J. Neurophysiol*. 86: 1445-1458, 2001.
39. Sinex, D.G. and Geisler, C.D. Auditory-nerve fiber responses to frequency-modulated tones. *Hearing Res*. 4: 127-148, 1981.
40. Suga, N. Responses of cortical auditory neurons to frequency modulated sounds in echo-locating bats. *Nature* 206: 890-891, 1965.
41. Suga, N., O'Neill, W.E., Kujirai, K. and Manabe, T. Specificity of combination-sensitive neurons for processing of complex biosonar signals in auditory cortex of the mustached bat. *J. Neurophysiol*. 49: 1573-1626, 1983.
42. Theunissen, F.E., Sen, K. and Doupe, A.J. Spectral-temporal receptive fields of nonlinear auditory neurons obtained using natural sounds. *J. Neurosci.* 20: 2315-2331, 2000.
43. Whitfield, I.C. and Evans, E.F. Responses of auditory cortical neurons to stimuli of changing frequency. *J. Neurophysiol*. 28: 655-672, 1965.
44. Whitsel, B.L., Dreyer, D.A. and Hollins, M. Representation of moving stimuli by somatosensory neurons. *Fed. Proc*. 37: 2223-2227, 1978.
45. Young, E.D. What's the best sound? *Science* 280: 1402-1403, 1998.